Maniatis, T., Fritsch, E. F., & Sambrook, J. (1982) *Molecular Cloning: A Laboratory Manual*, Cold Spring Harbor Laboratory, Cold Spring Harbor, NY.
Mathews, C. K., & Cohen, S. S. (1963) *J. Biol. Chem. 238*, 367-370.
Matthews, D. A., Appelt, K., & Oatley, S. J. (1989) *Adv. Enzyme Regul. 29*, 47-60.
Michaels, M. L., Kim, C. W., Matthews, D. A., & Miller, J. H. (1990) *Proc. Natl. Acad. Sci. U.S.A. 87*, 3957-3961.
Montfort, W. R., Perry, K. M., Fauman, E. B., Finer-Moore, J. S., Maley, G. F., Hardy, L., Maley, F., & Stroud, R. M. (1990) *Biochemistry 29*, 6964-6977.
Moore, M. A., Ahmed, F., & Dunlap, R. B. (1986) *J. Biol. Chem. 261*, 12745-12749.
Perry, K. M., Fauman, E. B., Finer-Moore, J. S., Montfort, W. R., Maley, G. F., Maley, F., & Stroud, R. M. (1990) *Proteins: Struct., Funct., Genet.* (in press).
Perryman, S. M., Rossana, C., Deng, T., Vanin, E. F., & Johnson, L. F. (1980) *Mol. Biol. Evol. 3*, 313-321.
Pinter, K., Davison, V. J., & Santi, D. V., (1988) *DNA 7*, 235-241.
Pogolotti, A. L., Jr., & Santi, D. V. (1977) in *Bioorganic Chemistry* (Van Tamelin, E., Ed.) Vol. I, pp 277-311, Academic Press, Orlando, FL.
Pogolotti, A. L., Jr., Ivanetich, K. M., Sommer, H., & Santi, D. V. (1976) *Biochem. Biophys. Res. Commun. 70*, 772-778.
Pogolotti, A. L., Jr., Weil, C., & Santi, D. V. (1979) *Biochemistry 18*, 2794-2804.
Pogolotti, A. L., Jr., Danenberg, P. V., & Santi, D. V. (1986) *J. Med. Chem. 29*, 478-482.
Richter, J., Puchtler, I., & Fleckenstein, B. (1988) *J. Virol. 62*, 3530-3535.
Rode, W., Scanlon, K. J., Hynes, J., & Bertino, J. R. (1979) *J. Biol. Chem. 254*, 11538-11543.
Sanger, F. (1981) *Science 214*, 1205-1210.
Santi, D. V., McHenry, C. S., & Sommer, H. (1974) *Biochemistry 13*, 471-481.
Santi, D. V., McHenry, C. S., Raines, R. T., & Ivanetich, K. M. (1987) *Biochemistry 26*, 8606-8613.
Santi, D. V., Pinter, K., Kealey, K., & Davisson, V. J. (1990) *J. Biol. Chem. 265*, 6770-6775.
Singer, S. C., Richards, C. A., Ferone, R., Benedict, D., & Ray, P. (1989) *J. Bacteriol. 171*, 1372-1378.
Takeishi, K., Kaneda, S., Ayusawa, D., Shimizu, K., Gotoh, O., & Seno, T. (1985) *Nucleic Acids Res. 13*, 2035-2043.
Taylor, J. W., Ott, J., & Eckstein, F. (1985) *Nucleic Acids Res. 13*, 8765-8785.
Taylor, G. R., Lagosky, P. A., Storms, R. K., & Haynes, R. H. (1987) *J. Biol. Chem. 262*, 5298-5307.
Thompson, R., Honess, R. W., Taylor, L., Moran, J., & Davison, A. J. (1987) *J. Gen. Virol. 68*, 1449-1455.
Wahba, A. J., & Friedkin, M. (1961) *J. Biol. Chem. 236*, PC11-12.
Weber, G. (1961) *Nature 190*, 27-29.
West, D. K., Belfort, M., Maley, G. F., & Maley, F. (1986) *J. Biol. Chem. 261*, 13446-13450.
Zoller, M. J., & Smith, M. (1984) *DNA 3*, 479-488.

Activator-Dependent Preinduction Binding of σ-70 RNA Polymerase at the Metal-Regulated *mer* Promoter†

Andreas Heltzel,‡ Ike Whan Lee, Paul A. Totis, and Anne O. Summers*
Department of Microbiology, University of Georgia, Athens, Georgia 30602
Received March 27, 1990; Revised Manuscript Received July 2, 1990

ABSTRACT: Expression of the Tn*21* mercury-resistance (*mer*) locus is controlled by the *merR* gene product, which represses *mer* structural gene (*merTPCAD*) transcription in the absence of mercuric ion [Hg(II)] and activates it in the presence of Hg(II). In vivo DNA methylation of the *mer* regulatory region (*merOP*) shows that, with or without the inducer Hg(II), MerR strongly protects four guanine residues in a dyadic region located between the −10 and −35 hexamers of the structural gene promoter (P_{TPCAD}). Prior to induction by Hg(II), RNA polymerase is also bound at P_{TPCAD}; occupancy of the uninduced promoter by RNA polymerase is dependent on MerR. Methylation and permanganate footprinting demonstrate that induction by Hg(II) results in MerR/Hg(II)-dependent promoter DNA melting in the −10 region of P_{TPCAD} and in additional DNA structural distortions within the region of dyad symmetry. Thus, MerR fosters the binding of RNA polymerase to an inactive promoter, and upon induction, MerR/Hg(II) facilitates DNA distortions suitable for efficient formation of the active transcription complex.

The bacterial mercury-resistance operon (*mer*) confers resistance to inorganic mercury [Hg(II)]. The most extensively studied examples of *mer* are encoded by the Gram-negative transposons Tn*21* and Tn*501* [reviewed in Summers (1986), Foster (1987), and Walsh et al. (1988)]. In Tn*21*, *mer* (Figure 1) consists of five structural genes encoding a Hg(II)-uptake system (*merT* and *merP*), the mercuric reductase enzyme (*merA*), and a small, low-abundance protein (*merD*) whose precise function is unknown (Lee et al., 1989). The role of an additional structural gene (*merC*), encoding an inner membrane protein present only in Tn*21*, has also yet to be established (Summers, 1986).

The expression of *merTPCAD* is under negative and positive control of the product of the *merR* gene (Figure 1; Foster et al., 1979; Ni'Bhriain et al., 1983; Foster & Brown, 1985; Lund et al., 1986; Heltzel et al., 1987). MerR also negatively

† This work was supported in part by a grant from the National Institutes of Health (GM28211).
* Correspondence should be addressed to this author.
‡ Present address: Zentrum für Molekulare Biologie, Universität Heidelberg, INF.282, D-6900 Heidelberg, Federal Republic of Germany.

0006-2960/90/0429-9572$02.50/0

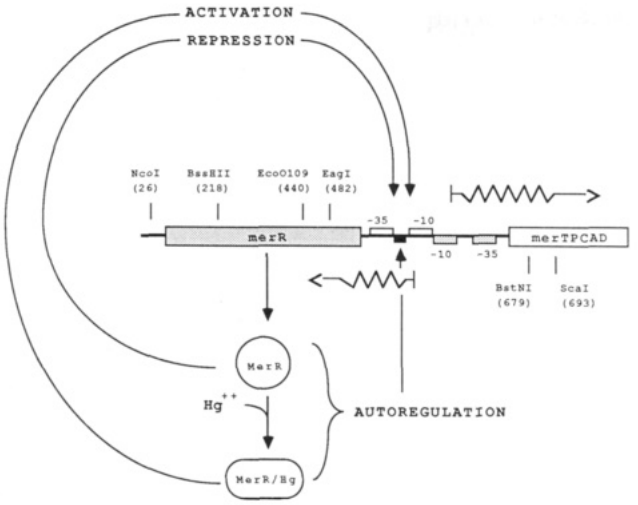

FIGURE 1: Structure and regulation of the *mer* operon of Tn*21*. The 667-bp *Nco*I–*Sca*I fragment present in pDG125 contains the divergently oriented promoters P_{TPCAD} and P_R with their respective −10 and −35 hexamers and their corresponding transcript origins (wavy lines). The in vitro MerR binding site between the −10 and −35 regions of P_{TPCAD} (O'Halloran et al., 1989; Shewchuk et al., 1989b; Heltzel et al., 1987) is indicated with a black bar, and relevant restriction sites are included according to the numbering system of Barrineau et al. (1984). The three known regulatory processes mediated by MerR [repression and activation of P_{TPCAD} and repression of P_R (Heltzel et al., 1987; Foster & Brown, 1985; Ni'Bhriain et al., 1983; Foster et al., 1979)] are indicated with solid arrows. The putative conformational change believed to occur in MerR is indicated by a circle (repressor) and an oval (activator) (Shewchuk et al., 1989a–c).

regulates its own synthesis independently of Hg(II) (Figure 1; Ni'Bhriain et al., 1983; Foster & Brown, 1985; Lund et al., 1986). In vitro MerR binds as a transcriptional repressor in the absence of Hg(II) and as an activator in the presence of Hg(II) to a symmetrical region within the overlapping divergent promoters P_{TPCAD}[1] and P_R (Heltzel et al., 1987; O'Halloran et al., 1989; Shewchuk et al., 1989b). This area of dyad symmetry (7-bp repeats separated by 4 bp) lies between the −10 and −35 hexamers of P_{TPCAD}.

MerR of Tn*21* differs from that of Tn*501* in only 9 out of 144 amino acids, and both proteins bind to identical DNA sequences in a completely conserved portion of the Tn*21* and Tn*501* regulatory sites (Heltzel et al., 1987; O'Halloran et al., 1989; Shewchuk et al., 1989b). Both P_R and P_{TPCAD} have extensive homology with the consensus *Escherichia coli* σ-70 promoter sequence (McClure, 1985) although the spacing between the respective −10 and −35 regions is unusually long (19 bp). The divergent transcripts originate 17 bp apart, and the untranslated 5′ end of *merR* mRNA overlaps the MerR binding site (Figures 1 and 3). Outside of the region of dyad symmetry, Tn*21* and Tn*501* differ by 30% in the untranslated 5′ end of the structural gene transcript (Barrineau et al., 1984; Misra et al., 1984). This 5′ untranslated region of *merTPCAD* mRNA is superimposed on the spacer and the −35 region of the divergent promoter for *merR* expression, P_R.

MerR suffices for transcriptional repression and Hg(II)-dependent activation of the Tn*501* *mer* structural genes in vitro (O'Halloran et al., 1989). Furthermore, when stimulating *mer* structural gene expression in vitro, MerR does not replace the normal σ-70 subunit of RNA polymerase (O'Halloran et al., 1989). Recent in vivo studies on the *mer* operons of Tn*21* (Ross et al., 1989) and of Tn*501* (Lund & Brown, 1987) show that none of the *mer* structural gene products is required for repression or transcriptional activation at the *mer* structural gene promoter.

Here we have analyzed in vivo transcription complexes engaged in the three known regulatory processes mediated by MerR at P_R and at P_{TPCAD}: repression of P_{TPCAD}, Hg(II)-dependent activation of P_{TPCAD}, and repression of P_R. We used dimethyl sulfate to detect the occupancy and shifts in occupancy of *merOP* DNA by MerR and RNA polymerase in the wild type, in a *merR* deletion mutant, and in a P_{TPCAD} down-promoter mutant. We also employed potassium permanganate in vivo to detect DNA melting associated with active transcription complexes in the wild-type and mutant strains. Our results clearly indicate that in vivo MerR fosters the binding of RNA polymerase at P_{TPCAD} even without Hg(II) induction and that active transcription from P_{TPCAD} is associated with structural distortions in the DNA on the 5′ side of the −10 hexamer, within the MerR binding site.

Materials and Methods

Bacterial Strains and Plasmids. The bacterial host strain used was SK1592 (*gal*, *thi*, *sbcB*15, *endA*, *hsdR*4; Kushner, 1978). Plasmid pDG125 carrying wild-type *merR*, the *mer* operator–promoter (*merOP*), and the first 89 bp of *merT* on a 667 base pair (bp) *Nco*I–*Sca*I fragment has been described (Heltzel et al., 1987). A *merR* deletion mutant (pAH1974; elsewhere referred to as *merR*Δ) was constructed from pDG125 by deleting *merR* leftward from the *Eag*I site (Heltzel et al., 1989). This *merR*Δ construct resulted in a truncated *merR* gene (17 amino acids) with an additional 25 nonspecific amino acids (from pT7-3) upstream from the *Nco*I site before termination at a TGA codon in frame with *merR*. Plasmid pAH1989, carrying the *mer* *Nco*I–*Sca*I fragment (Figure 1) with a G-C to A-T transition (generated by treatment with hydroxylamine; Ross et al., 1989) at the −36 position of the P_{TPCAD} promoter (elsewhere referred to as the $G_{-36}A$ mutant), was derived by insertion of a 687-bp *Hin*dIII–*Bam*HI fragment from pSJ61 [S.-J. Park, personal communication; the *mer* *Nco*I–*Sca*I $G_{-36}A$ fragment of pSJ61 was derived from pWR126 (Ross et al., 1989)] into pT7-3 digested with *Hin*dIII and *Bam*HI at the polylinker site.

In Vivo Methylation. Cells containing one of the above plasmids were grown at 37 °C with aeration in minimal A medium (Miller, 1972) supplemented with glucose (0.5%), thiamin hydrochloride (0.001%), and 25 μg of ampicillin per milliliter. Exponential-phase cells were harvested as 100-mL aliquots at 5000 rpm for 5 min. After 100-fold concentration in fresh minimal media, cells were transferred to a 37 °C water bath. Cells were induced, where indicated, with 1 μM mercuric chloride ($HgCl_2$; complexed with 2 μM glutathione) for 60 s before being methylated [the maximum transcription rate of P_{TPCAD}, 35–40 n/s, occurs within 1 min after Hg(II) induction (Gambill and Summers, unpublished results)]. Rifampicin- (200 μg/mL) treated cells were exposed only to rifampicin or simultaneously to $HgCl_2$ and rifampicin for 30 min prior to methylation. Rifampicin concentration and length of treatment were adapted from Borowiec and Gralla (1986) and are the optimal conditions for "freezing" RNA polymerase at a promoter. Five microliters of dimethyl sulfate (DMS, Aldrich) was added (0.5%), and incubation was continued for 30 s with shaking. The reaction was stopped by pouring the samples over 5 g of ice and adding 20 mL of ice-cold EN buffer (0.25 M EDTA, pH 8, 0.1 M NaCl). After centrifugation, the cell pellets were washed once with TEN buffer

[1] Abbreviations: DMS, dimethyl sulfate; EDTA, ethylenediaminetetraacetate; *lacZ*, β-galactosidase; *merOP*, divergent *mer* operator–promoter region; P_R, promoter for *merR*; P_{TPCAD}, promoter for *merTPCAD*; SDS, sodium dodecyl sulfate; Tris-HCl, tris(hydroxymethyl)aminomethane hydrochloride.

(Giniger et al., 1985) and stored at −20 °C.

Nuclease End Mapping of the merR and merTPCAD Transcripts. Nuclease end mapping was carried out as described by Maniatis et al. (1982) except that mung bean nuclease (100 units/mL, Promega Biotech.) was used to remove single-stranded DNA overhangs. RNA was prepared from SK1592 (pAH1974) by harvesting 100 mL of exponential-phase cells. The cell pellet was suspended in 1/28 volume M9 buffer (Miller, 1972) containing 10 mM sodium azide. This cell suspension was extracted twice with phenol–1% sodium dodecyl sulfate and once with chloroform–isoamyl alcohol (24:1 v/v), and finally, the RNA was precipitated with 2.5 M lithium chloride at −20 °C. RNA precipitates were collected by centrifugation, washed twice with 70% ethanol, and suspended in sterile, diethyl pyrocarbonate treated water to a final concentration of ca. 1 μg/mL. The DNA target fragment for 5′ end mapping of *merR* was *Eco*O109–*Bst*NI (239 bp; Figure 1) labeled at the *Eco*O109 site with T4 polynucleotide kinase (New England Biolabs), and for mapping of the *merTPCAD* 5′ end, this fragment was labeled at the *Bst*N1 site with T4 polynucleotide kinase.

In Vivo Treatment with Potassium Permanganate. Cells were grown to exponential phase as described above. Twenty-five milliliter aliquots of uninduced or 1 μM $HgCl_2$ induced cells were either immediately exposed to potassium permanganate ($KMnO_4$, 6.25 mM; J. D. Gralla, personal communication) or treated for 5 min with 200 μg/mL rifampicin [rifampicin conditions were adapted from Sasse-Dwight and Gralla (1988)] prior to $KMnO_4$ exposure for 4 min at 37 °C with shaking. After $KMnO_4$ treatment, cells were immediately placed on ice, harvested at 4 °C, and stored at −20 °C.

Analysis of Modified Plasmid DNA. Cells were lysed as described by Crosa and Falkow (1981). Plasmid DNA modified with DMS or $KMnO_4$ was extracted once each with buffer-saturated phenol–chloroform (1:1 v/v) and chloroform–isoamyl alcohol (24:1 v/v). Heat-inactivated DNase-free RNase (10 μL; 10 mg/mL) was added, and the samples were incubated for 30 min at 37 °C prior to phenol–chloroform extraction. The DNA was ethanol precipitated and suspended in deionized water. $KMnO_4$-treated DNA was further purified by filtration through a G-50 spin column (5 Prime → 3 Prime, Inc.), and the DNA was precipitated from the effluent with ethanol and sodium acetate (0.3 M, pH 7), washed once with ethanol, dried, and then suspended in water.

Plasmid DNA was digested with *Eco*O109 and *Bst*NI (for pDG125 and pAH1989) or with *Hin*dIII and *Bst*NI (for pAH1974) according to the specifications of the enzyme vendors. After electrophoresis the *merOP* fragments (*Eco*O109/*Bst*NI = 239 bp or *Hin*dIII/*Bst*NI = 235 bp) were excised, electroluted, ethanol precipitated, and suspended in water. The 3′ termini were labeled with either [α-^{32}P]TTP (3′ terminus of *Bst*NI; top strand) or [α-^{32}P]dCTP (3′ termini of *Eco*O109 or *Hin*dIII sites; bottom strand) by use of DNA polymerase/Klenow (1 unit, Pharmacia). DNA treated with $KMnO_4$ was, prior to strand cleavage, denatured by exposure to 1 mM NaOH for 2 min at 80 °C, reprecipitated with ethanol, washed once, and dried. In order to cleave the labeled fragments at modified bases, the DNA pellets were suspended in 100 μL of 1 M piperidine and incubated in screw-cap tubes for 30 min at 90 °C. Piperidine was removed by lyophilization; the pellets were washed twice in 100 μL of water and dried. Cleaved DNA was electrophoresed on 8% denaturing polyacrylamide–urea sequencing gels (Maxam & Gilbert, 1980). Gels were vacuum dried with heat onto filter paper (Whatman 3MM) and exposed with intensifying screens at −70 °C on Kodak X-Omat AR film for various lengths of time.

Densitometry. Autoradiographs were scanned from position −48 to position +26 with a Zeineh soft laser scanning densitometer (Model SL-TRFF) and analyzed on an Apple IIe computer with integration software developed by Biomed Instruments Inc., Fullerton, CA. Rather than to choose arbitrarily a single reference band whose intensity we assume is never affected by different experimental conditions, the intensity (peak area) of all bands from position −48 to position +26 of each lane was summed, and each band was normalized to the total lane intensity. For quantitative comparison, each band's normalized value was compared to that of the corresponding in vitro G band since the methylation pattern of the in vitro G reaction consistently resembled that of the in vivo methylated DNA from the *merR* deletion mutant pAH1974 in the absence of rifampicin and/or Hg(II) (see Results). In other words, there was close correspondence between the in vitro G methylation pattern and the in vivo methylation pattern of a nonfunctional *mer* structural gene promoter (P_{TPCAD}).

RESULTS

MerR Occupies the Same Site in Vivo Regardless of Whether the Inducer Hg(II) Is Present or Not. In vitro and in vivo DMS treatment of protein–DNA complexes is a useful tool for the identification of nucleic acid sites that are occupied by DNA binding proteins. Such protected DNA sites can be identified through the ability of a bound protein to alter the access of DMS to the reactive positions of nucleotides within its DNA binding site. On double-stranded DNA, DMS methylates the N-7 (major groove) of guanine and the N-3 (minor groove) of adenine (Lawley & Brookes, 1963). The N-1 of adenine and the N-3 of cytosine can also be methylated when these bases are not hydrogen-bonded to their complementary bases (Lawley & Brookes, 1963).

Densitometric analysis of the DNA methylation pattern of the *mer* regulatory region (*Eco*O109 to *Bst*NI, Figure 1) of pDG125 (*merR*$^+$; Figure 2, lanes 1–4) revealed strong protection [compared to the corresponding in vitro G reaction (Figure 2, lane 9)] of two guanines on the top (−18, −30) and on the bottom (−19, −31) strands in the dyadic region of P_{TPCAD} (unless otherwise indicated, base positions are with respect to +1 of the *merTPCAD* start site). The lack of protection at these positions in the *merR* deletion mutant, pAH1974 (*merR*Δ; Figure 2, lanes 5–8), demonstrated that these G protections are MerR dependent. The four protected G's are separated by 11 bp and would lie approximately on the same face of a B-DNA helix (Figure 9). DMS treatment of the *merR*$^+$ strain in the absence or presence of Hg(II) and/or rifampicin (Figure 2, lanes 2–4) did not alter the methylation patterns of G's at −30 (top) or −19 and −31 (bottom). However G −18 (top), which is located nearest to the −10 region of P_{TPCAD} (Figure 3), was less protected in the presence of Hg(II)/rifampicin (Figure 2, lane 4) than it was in DNA from nontreated cells (Figure 2, lane 1) or in DNA from cells treated with Hg(II) alone or with rifampicin alone (Figure 2, lanes 2 and 3; see also Figure 3). In addition, symmetrically located adenines −16 (top) and −33 (bottom) (Figure 2) showed MerR-dependent Hg(II)- and rifampicin-independent methylation enhancements compared to DNA from *merR*Δ cells and to DNA methylated in vitro (Figure 2, lanes 5–9). The four in vivo G protections correspond precisely to those attributed to MerR occupancy in the in vitro DNA footprint analysis of the homologous Tn*501* MerR/*merOP* interaction (O'Halloran et al., 1989; Shewchuk et al., 1989b). However, additional methylation protections and enhancements upstream of the site bound by MerR (O'Hal-

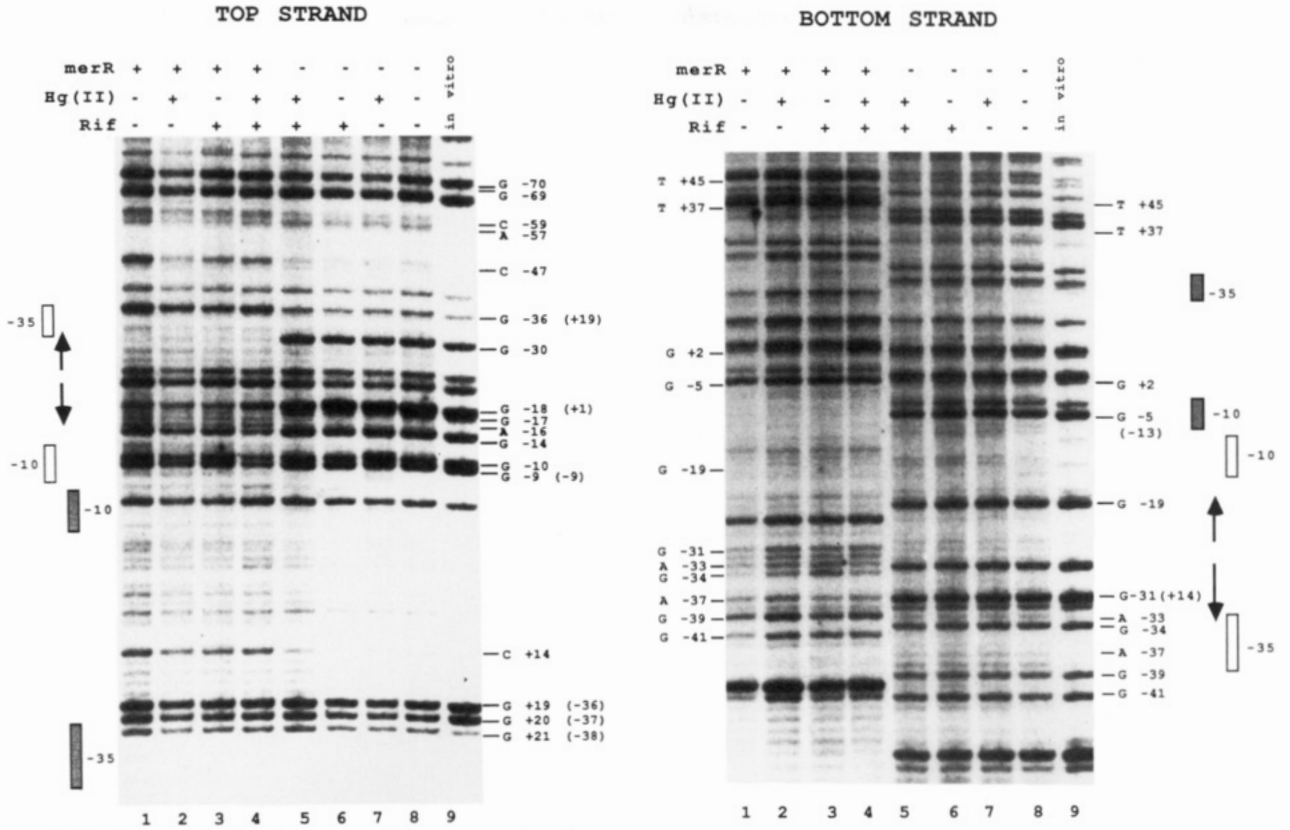

FIGURE 2: In vivo methylation of the top and bottom strands of the *mer* regulatory region from wild-type pDG125 (lanes 1–4) and of the *merR* deletion mutant pAH1974 (lanes 5–8) in the absence or presence of Hg(II) and/or rifampicin (Rif). Lane 9, in vitro G reaction. Nucleotide numbering is with respect to +1 of the *merTPCAD* transcript, and the numbers in brackets correspond to +1 of the *merR* transcript. Open and shaded bars indicate the −10 and −35 regions of P_{TPCAD} and P_R, respectively. Solid arrows indicate the region of dyad symmetry.

loran et al., 1989) suggested that in vivo, even in the absence of inducer [Hg(II)], this region is occupied by more than just MerR.

MerR Promotes RNA Polymerase Binding to P_{TPCAD} Prior to Induction. The MerR binding site is flanked by the σ-70 RNA polymerase recognition elements (−10 and −35 regions) of the P_{TPCAD} promoter (Figure 1). While one might expect that MerR functioning as a repressor [in the absence of Hg(II)] would exclude RNA polymerase from these sites, the similarity of the methylation changes in the −35 region of *merOP* to those identified with RNA polymerase occupancy in other systems (Siebenlist et al., 1980; Kirkegaard et al., 1983; Borowiec & Gralla, 1986; Shanblatt & Revzin, 1986) suggested RNA polymerase occupancy at P_{TPCAD}. Specifically, we observed, in the absence of Hg(II), prominent differences in methylation of highly conserved bases (McClure, 1985) in the −35 region of P_{TPCAD} in *merR*$^+$ strains compared to *merR*Δ strains. In a *merR*$^+$ background, the G at position −34 (bottom) was protected, and G −36 (top) and A −37 (bottom) were hyperreactive (Figure 2, compare lane 1 with lanes 8 and 9 containing *merR*Δ and in vitro G reactions, respectively). These −35 region protections and enhancements also correspond to those attributed to RNA polymerase occupancy in the in vitro footprinting of Tn*501 merOP*; however, in that system, RNA polymerase binds to the MerR–*merOP* linear DNA complex only after Hg(II) is added (O'Halloran et al., 1989).

Further evidence that these DMS reactions in the −35 region of uninduced P_{TPCAD} result from the presence of RNA polymerase can be seen in the effect of rifampicin treatment on the in vivo *merOP* footprint. Rifampicin prevents transcription initiation in vitro without affecting the formation of open promoter complexes (Sippel & Hartmann, 1968; Carpousis & Gralla, 1985), and in vivo rifampicin strengthening of certain methylation protections in the *lacUV5* system is thought to result from rifampicin "freezing" RNA polymerase at the promoter (Borowiec & Gralla, 1986). Thus, rifampicin-induced methylation changes in DNA footprints can be ascribed to RNA polymerase occupancy, although absence of a rifampicin-associated change does not rule out an interaction with RNA polymerase. Even in the absence of Hg(II), G −36 (top strand) remained generally hyperreactive with rifampicin while the methylation intensity of G −34 and A −37 (bottom strand) was unaffected by rifampicin treatment (Figure 2, compare lanes 1 and 3; see also Figure 3). Since we know from the in vitro studies of O'Halloran et al. (1989) that these three bases are not affected by MerR alone and since we expect on the basis of other studies (Siebenlist et al., 1980; Sasse-Dwight & Gralla, 1988, 1989) that the reactivity of these bases would be emphasized by rifampicin-provoked freezing of RNA polymerase, the fact that G −36 (top) and G −34 and A −37 (bottom) retain their characteristic hypersensitivity or protection with or without rifampicin is consistent with RNA polymerase occupying that region at the same level both before and after the inducer Hg(II) is added.

To substantiate this unexpected finding, we examined the methylation of an activation-deficient mutant (pAH1989) which has a strong down-promoter mutation in the highly conserved −35 region of P_{TPCAD} (G_{-36} A derived from pWR126; Ross et al., 1989; see below). With pAH1989 we expected to see the retention of methylation protections in the dyadic MerR binding region and the absence of methylation protections/enhancements in the −35 region indicating failure of RNA polymerase to occupy this region. The DNA methylation pattern of *merOP* in this G_{-36} A mutant showed that MerR protection of G's −18, −19, −30, and −31 and hyper-

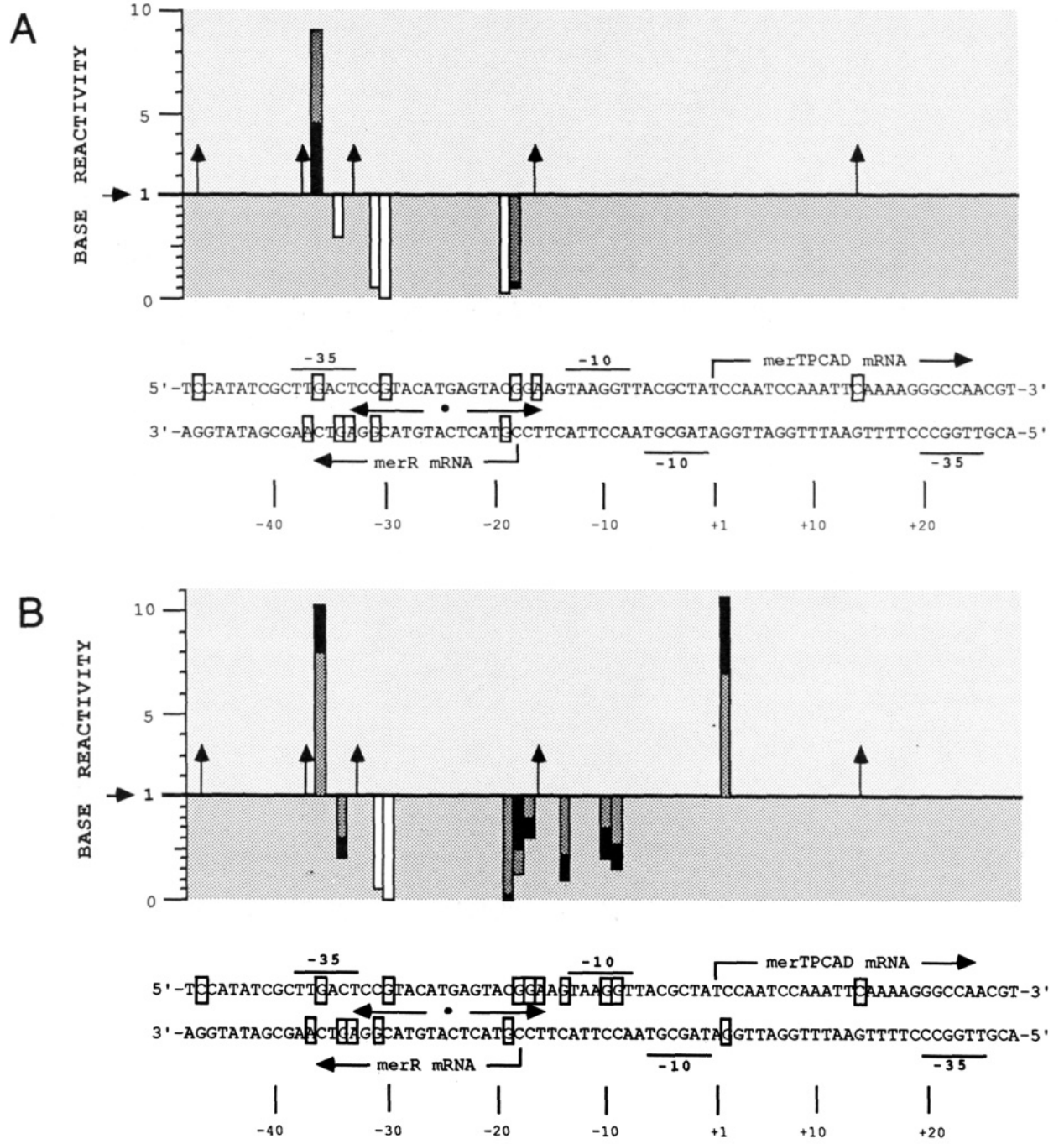

FIGURE 3: Summary of the normalized methylation patterns of wild-type pDG125 DNA from position −48 to position +26 [(A) absence of Hg(II); (B) presence of Hg(II)] compared to the respective normalized in vitro G control. Changes in boxed bases in the sequence are depicted by bars or arrows in the graph. The horizontal axis (at 1) indicates the relative methylation of each base in the in vitro G reactions. Values of >1 (above solid line) designate hyperreactivities (*x*-fold) whereas values of <1 indicate degree of protection (complete protection = 0). Arrows indicate hyperreactivities of bases other than G's. Shaded and black bars depict base reactivities in the absence and presence of rifampicin, respectively. Open bars designate identical base reactivities ± rifampicin.

reactivities of A's −16 and −33 were identical with those in the wild-type *merR* strain (Figure 4, compare lanes 1 and 3 with lane 6). Thus, MerR protects the same dyadic region in this activation-deficient mutant as it does in wild-type P_{TPCAD} DNA. In contrast, G −34 (bottom) is not protected, and A −37 (bottom) is not hyperreactive (Figure 4, compare uninduced lanes 3 and 6 and induced lanes 4 and 5; note also Figure 2, lanes 6 and 8, for behavior of the wild-type P_{TPCAD} in the *merR*Δ background). Thus, the genetic data support the case made by homology with other promoters and by consistency with in vitro *mer* footprinting that these Hg-independent methylation enhancements and protections in the −35 region are caused by RNA polymerase binding.

The question of whether RNA polymerase and MerR are binding alternatively or simultaneously was resolved as follows. With in vivo footprinting [as with solution footprinting in vitro (Straney & Crothers, 1987)] a pattern suggesting simultaneous occupancy of DNA by two or more proteins could also arise from a mixed population in which the proteins alternatively occupy their respective sites. Thus, in in vitro footprinting, it is essential to separate multiprotein–DNA complexes by electrophoresis before footprinting them. Since prior physical separation of complexes is not possible with in vivo footprinting, other arguments must be invoked to support simultaneous occupancy. In the case of the *mer* operon, there is extensive evidence that, in *merR*$^+$ strains without the inducer Hg^{2+}, the

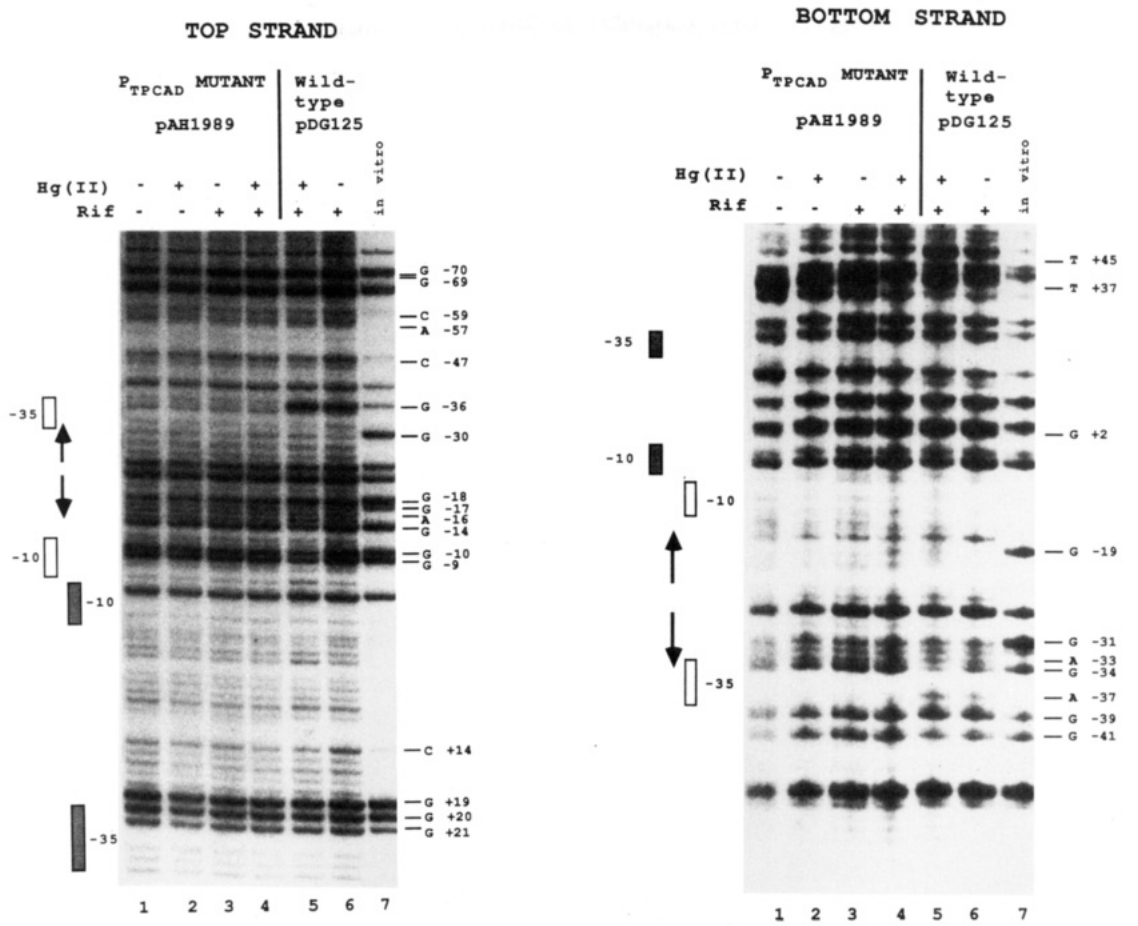

FIGURE 4: In vivo methylation pattern (top and bottom strand) of wild-type [Rif and Hg(II)/Rif only; lanes 5 and 6] and the $G_{-36}A$ mutant (lanes 1–4). Landmark elements of the *mer* regulatory region are indicated as in Figure 2.

level of transcription is 100–200-fold lower than in the fully induced state. Moreover, in a *merRΔ* (permanently derepressed) strain, transcription occurs at approximately 10% of the fully induced *merR*$^+$ state (Ross et al., 1989). To substantiate that the pDG125-based system used for footprinting was behaving similarly, we determined the level of *mer*-specific 5′ mRNA produced in cells containing either pDG125 or the *merRΔ* derivative, pAH1974, under inducing and noninducing conditions (Figure 5). In the wild-type *merR* strain (carrying pDG125) *mer*-specific mRNA was not detectable without added Hg(II) (Figure 5, fifth lane). However, both 5 and 1 μM $HgCl_2$ provoked abundant synthesis of *mer* mRNA (Figure 5, third and fourth lanes) in pDG125-containing strains. The derepressed level of *mer* mRNA seen in pAH1974 (Figure 5, sixth lane) is roughly 10% (densitometrically; not shown) of the fully induced level (1 μM). Recall that in footprints described above, no occupancy by either *merR* or RNA polymerase is detectable in pAH1974 under any conditions. Thus, although derepressed transcription is easily detectable with the nuclease end mapping method, the sensitivity of footprinting is insufficient to demonstrate occupancy of the derepressed *mer* structural gene promoter by RNA polymerase alone (Figure 2, compare lanes 5–8 with lane 9). If the footprint of uninduced wild-type *merR–merOP* had arisen from a mixture of promoters with some carrying RNA polymerase alone and the rest carrying MerR alone, we would expect to see at least some transcription in the repressed state, but we see none (Figure 5, fifth lane). Since the intensities of the protections and enhancements in the −35 region ascribed to RNA polymerase change very little upon addition of Hg(II) (Figure 2, lanes 1–4, and Figure 3), but transcription only occurs with Hg(II), we conclude that MerR and RNA polymerase bind simultaneously to *merOP* both before and after induction by Hg(II).

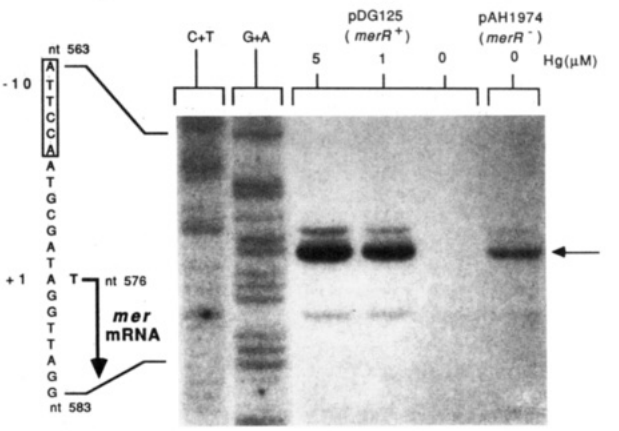

FIGURE 5: Nuclease 5′ end mapping of the *merTPCAD* transcript. The fragment marked by the arrow represents the 5′ end of the *merTPCAD* transcript corresponding to nt 576. This assignment takes into account the ca. 1.5-nucleotide difference between ends mapped by nuclease protection and by chemical sequencing (Aiba, 1983; Green & Roeder, 1980). The sequence of the bottom strand from standard sequencing reactions C+T and G+A (Maxam & Gilbert, 1980) is shown on the left including the −10 hexamer (white bar) of P_{TPCAD}.

Activation of P_{TPCAD} Involves a MerR/Hg(II)-Dependent Rearrangement of Bound RNA Polymerase. Upon induction with Hg(II), MerR-dependent methylation of certain bases in wild-type *merOP* changed markedly while that of others was unaltered. Of the G's protected by MerR [−18 and −30 (top) and −19 and −31 (bottom)], only G −18 was less protected when induced (Figure 2, lanes 1–4, and densitometric analysis, Figure 3). Of the G's in the −35 region which we

believe are interacting with RNA polymerase, G −34 (bottom) was more protected and G −36 (top) became more hyperreactive in response to Hg(II) (Figure 2, lanes 2 and 4, and Figure 3). Protection of G's at −17, −14, −10, and −9 (top strand) increased markedly in the presence of Hg(II), and their protection was strengthened with rifampicin treatment (Figure 2, lanes 2 and 4, and Figure 3). A Hg(II)/MerR-dependent hypermethylation occurred at G +2 (bottom), and the reactivity of this base was further increased with rifampicin (Figure 2, lanes 2 and 4, and Figure 3B). In the activation-deficient mutant $G_{-36}A$ (pAH1989) and in the *merR*Δ mutant (pAH1974), these Hg(II)-dependent changes in DMS reactivity were absent (Figure 2, compare lanes 2 and 4 with lanes 5 and 7; also Figure 4, lanes 2, 4, 5, and 6).

The protected G's (−10 and −9 on the top strand) and the hyperreactive G +2 (bottom strand) are located downstream of the MerR binding site and would lie on the same helical face as the MerR-protected bases (Figure 9B); however, G's −17 and −14 do not lie on the same helical face occupied by MerR. We believe methylation changes at these positions arise from RNA polymerase beginning transcription at P_{TPCAD}. The assignment of these in vivo DMS reactions to RNA polymerase occupancy during Hg(II) induction corresponds to the assignment of these positions as the in vitro Hg(II)/MerR-dependent RNA polymerase footprint at P_{TPAD} in Tn*501* (O'Halloran et al., 1989).

Methylation enhancements outside of the regions of P_{TPCAD} occupied by MerR or by RNA polymerase were more extensive than those observed in the in vitro system (O'Halloran et al., 1989). Hg(II)-independent hyperreaction was found at C's −47 and +14 (top) in *merR*$^+$ but not in *merR*Δ (Figure 2, compare lanes 1–4 with lanes 5–8). Of these bases in the $G_{-36}A$ mutant, C −47 displayed slight hyperreactivity whereas C +14 was slightly hyperreactive only when treated with rifampicin alone (Figure 4, compare lanes 1–4 with lanes 5 and 6). We also observed DMS reaction in two distant downstream T's (probably +45 and +37, bottom) in *merR*$^+$ which were not seen in *merR*Δ (Figure 2, compare lanes 1–4 with lanes 5–8). In the $G_{-36}A$ mutant, DMS hyperreaction of T +45 was not observed, whereas T +37 was hyperreactive unless treated with Hg(II) and rifampicin (Figure 4, compare lanes 1–3 with lane 4; see also lanes 5 and 6 containing *merR*$^+$). The reactive site or sites of DMS methylation on T residues are not known; however, Sasse-Dwight and Gralla (1989) have observed DMS-reactive T's both in vitro and in vivo. Hyperreactions compared to the in vitro G reactions were also detected at C −59 and A −57 (top strand) in *merR*$^+$, *merR*Δ, and $G_{-36}A$ DNAs (Figure 2, compare lanes 1–8 with lane 9; Figure 4, compare lanes 1–6 with lane 7). Since these changes occur in wild-type and in both mutants, they cannot be unequivocally assigned to the MerR and/or RNA polymerase interaction at *merOP*; however, they indicate that in the in vivo supercoiled state there are some striking deviations in the methylation pattern of this region compared to that observed in vitro. The relevance of these more distant DMS reactions to *mer* operon function is being explored genetically.

Hg(II)-Dependent Transcription Is Associated with Helix Distortions within and Upstream of the −10 Region of P_{TPCAD}. Helix melting associated with transcriptional activity of a promoter can be detected in vitro and in vivo with $KMnO_4$ which reacts preferentially with unpaired thymines and cytosines (Borowiec et al., 1987; Sasse-Dwight & Gralla, 1989). Therefore, $KMnO_4$ treatment in vivo permits the observation of promoter DNA melted by RNA polymerase in an open complex (Sasse-Dwight & Gralla, 1989). As noted above, the signal intensity of melted promoter DNA is strongly enhanced by rifampicin, which traps RNA polymerase–promoter complexes (Sasse-Dwight & Gralla, 1988, 1989). $KMnO_4$ has also been used in vitro to detect helical distortions associated with sharp DNA bends (Borowiec et al., 1987).

In the region between −13 and +1 of P_{TPCAD}, treatment with Hg(II) and rifampicin, as compared to rifampicin only, resulted in strong $KMnO_4$ reactions at thymines on the top (−13, −7, −2, and +1) and on the bottom strands (−12) of *merR*$^+$ DNA (Figure 6, lanes 4 and 5). These Hg(II)/rifampicin-dependent $KMnO_4$ reactions in a region known to be melted during open complex formation in other promoters (Siebenlist, 1979; Siebenlist et al., 1980; Kirkegaard et al., 1983; Sasse-Dwight & Gralla, 1988, 1989) were not seen in $KMnO_4$-treated DNA of the *merR*Δ mutant (Figure 6, lanes 6 and 7) or of the $G_{-36}A$ mutant (Figure 7, lanes 3 and 4 and lanes 7 and 8). The identification of these bases as being involved in open complex at P_{TPCAD} is consistent with in vitro observations (O'Halloran et al., 1989). However, we did not detect $KMnO_4$-hyperreactivity in vivo at T −8 (top strand) and at T's −11, −6, and −1 (bottom) (Figure 6, lanes 4 and 5), whereas in the in vitro Tn*501* system all nine T's in this region were melted upon induction. It may be that the reactivity of certain T's is modulated differently by supercoiling in one system than in another; for example, in the *lac* system, the open complex pattern obtained with $KMnO_4$ in vivo and in vitro on supercoiled DNA was identical, though several T residues in the region were also not reactive in either condition (Sasse-Dwight & Gralla, 1989).

We also observed Hg(II)/rifampicin-dependent $KMnO_4$ reactions outside of the region typically melted by RNA polymerase in an open complex. On the bottom strand, T −20 and T −26 and, surprisingly, G −31 and A −33 became hyperreactive to $KMnO_4$ in the presence of Hg(II) and rifampicin (Figure 6, lanes 2–5). These bases lie within the region of dyad symmetry (Figure 9B), and their $KMnO_4$ reactivity (G −31 and A −33) or hyperreactivity (T −20 and T −26) was not seen in the *merR*Δ or the $G_{-36}A$ DNAs (Figure 6, lanes 6–9, and Figure 7). Thus, activation of P_{TPCAD} is accompanied by structural distortions in the DNA to which MerR is bound, ranging from 7 to 20 bases upstream of the region typically associated with open complex formation by RNA polymerase (Figure 9B).

In vivo $KMnO_4$ footprints typically have a higher and more variable background of T reactions than the in vitro $KMnO_4$ footprints (Sasse-Dwight & Gralla, 1989). Thus, increases in T reactivity are generally considered relevant only if they occur upon rifampicin treatment, the assumption being that they arise from the "stalling" of RNA polymerase in the open complex configuration. Nonetheless, we noted in the wild-type *merR* strain some T's whose reactivity increased in the presence of Hg(II) alone, but which remained relatively unreactive when treated with both rifampicin and Hg(II) (compared to treatment with rifampicin alone). For example (Figure 6, bottom strand), the reactivity of T's at −16, −23, −28, −35, −43, and −45 and C's at −17 and −24 appears Hg(II) inducible but is not enhanced (compared to T −12) by the addition of both Hg(II) and rifampicin. While neither mutant showed the prominent increases in T reactivity seen in the wild type upon induction, some of these Hg(II)-inducible, rifampicin-dampened increases in T reactivity were also seen in the *merR*Δ mutant (Figure 6, bottom strand; T's −12, −16, −35, and −43) and in the $G_{-36}A$ mutant (Figure 7, bottom stand; T's −12, −16, −20, and −28). The $G_{-36}A$ down-promoter mutant lacked the atypical G −31 and A −33 (bottom) reactions, and the

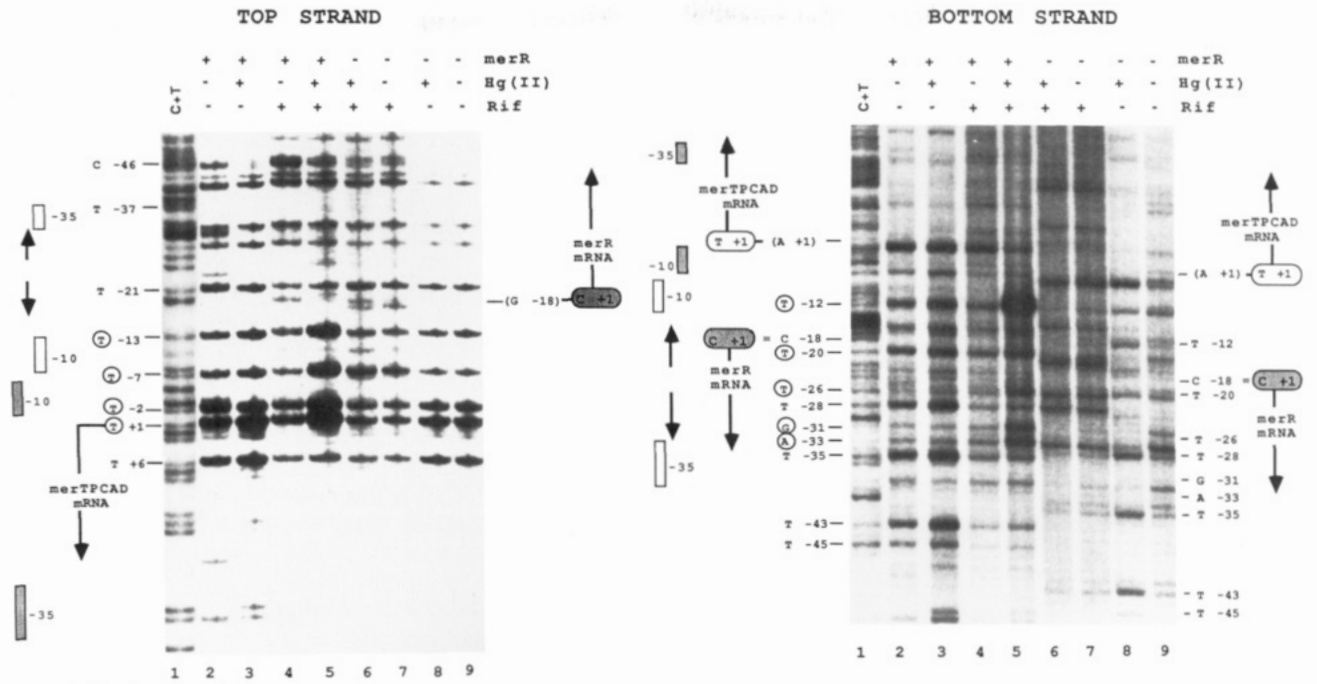

FIGURE 6: In vivo $KMnO_4$ treatment of the *mer* regulatory region (top and bottom strands) from wild-type pDG125 (lanes 2–5) and the *merR* deletion mutant pAH1974 (lanes 6–9) in the absence or presence of Hg(II) and/or rifampicin (Rif). Lane 1, in vitro C+T reaction. Nucleotide numbering is with repect to +1 of the *merTPCAD* message start, and the −10 and −35 regions of P_{TPCAD} and P_R are indicated with open and shaded bars, respectively. The positions of $KMnO_4$-reactive bases are indicated. Hg(II)/Rif-dependent hyperreactive bases are circled (see text).

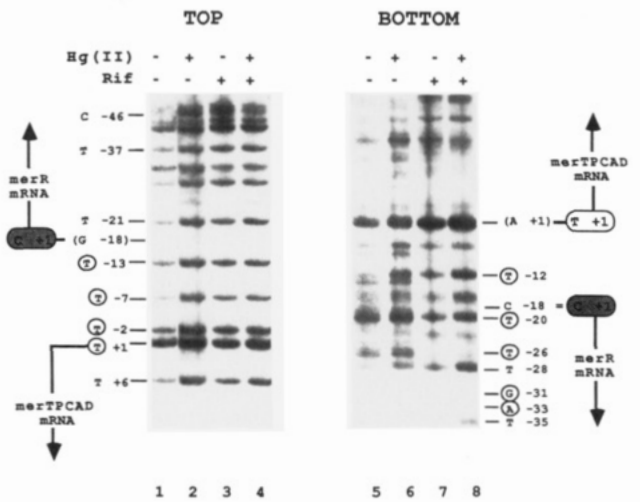

FIGURE 7: In vivo $KMnO_4$ reaction pattern of the $G_{-36}A$ mutant (top and bottom strands). Circled bases correspond to the Hg(II)/Rif-dependent hyperreactive residues seen in wild-type *mer* DNA (Figure 6).

reactivity of the T at −26 was markedly diminished by rifampicin treatment. Finally, the T at −37 (top) is quite reactive in the $G_{-36}A$ mutant (Figure 7) but not in either $merR^+$ or *merR*Δ (Figure 6, top). Possible causes for these atypical T reactions, which occur only on the bottom strand, will be considered below.

RNA Polymerase Footprint at Transcriptionally Active P_R Is Less Distinct in Vivo Than That of P_{TPCAD}. Since transcriptional and translational *lacZ* fusions in *merR* (Foster & Brown, 1985; Heltzel et al., unpublished observations) and in vitro run-off transcription with purified proteins (O'Halloran et al., 1989) have shown that MerR represses its own synthesis severalfold, independently of Hg(II), deletion of *merR* is expected to increase transcriptional activity from P_R. The footprints of plasmid pAH1974 containing the *mer* regulatory region with a truncated, biologically inactive *merR* gene (Ross et al., 1989) were examined for evidence of RNA polymerase occupancy of P_R in vivo.

Densitometry of the DNA methylation patterns at P_R indicated that, with or without rifampicin, differences in methylation associated with possible RNA polymerase binding at P_R are small. Slight protections occurred at positions (with respect to the *merR* transcript start site at +1) −37, −36 and −9 (top) and −13 and +14 (bottom); slight hypermethylations were seen at −38, +1, and +19 (top) (Figure 2, compare lanes 6 and 8 with lane 9 containing in vitro G reactions). In the $merR^+$ strain these putative RNA polymerase associated changes at P_R are absent (Figure 2, compare lanes 1 and 3). These protections and hypermethylations in *merOP* may be masked in the $merR^+$ strain by MerR or by RNA polymerase bound at P_{TPCAD}. For Tn*501*, O'Halloran et al. (1989) observed a distinct RNA polymerase protection pattern in vitro on linear DNA at P_R in the absence of MerR. However, due to sequence differences in this region of Tn*21* and Tn*501* (Barrineau et al., 1984; Misra et al., 1984), the RNA polymerase caused footprints at P_R may not be strictly comparable in these two systems.

Since the $KMnO_4$ reaction pattern of *merR*Δ DNA also did not indicate open complex related melting in the presence of rifampicin (Figure 6, compare lanes 7 and 9), we verified that P_R was active in pAH1974 in vivo by mapping the 5′ end of the *merR* transcript in aliquots of *merR*Δ cells removed just prior to DMS treatment (Figure 8). With the 1.5-nucleotide adjustment to compensate for the difference in the ends as determined by nuclease protection and by chemical sequencing (Aiba, 1983; Green & Roeder, 1980), we find that the Tn*21* *merR* transcript starts at nucleotide 558 (C), which corresponds exactly to the *merR* transcript start in Tn*501* (574 C; Lund et al., 1986; O'Halloran et al., 1989). Thus, the *merR* promoter is active; however, the $KMnO_4$ footprinting results suggest that, even in the presence of rifampicin, in vivo melting of P_R as an open complex is sufficiently transient as to limit its detection. Possible reasons for the differences in the sus-

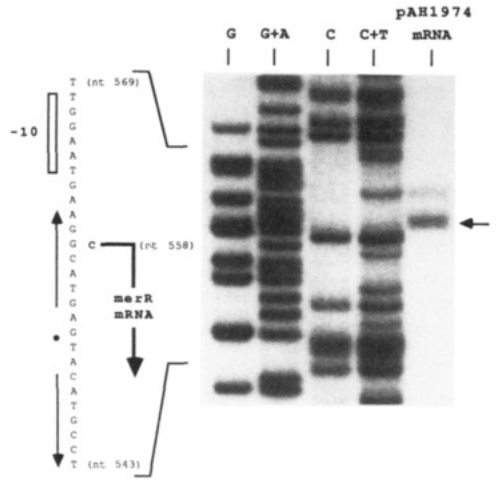

FIGURE 8: Nuclease 5′ end mapping of the *merR* transcript. The fragment marked by the arrow represents the 5′ end of the *merR* transcript corresponding to nt 558. This assignment takes into account the ca. 1.5-nucleotide difference between ends mapped by nuclease protection and by chemical sequencing (Aiba, 1983; Green & Roeder, 1980). The sequence of the top strand from standard sequencing reactions G, G+A, C, and C+T (Maxam & Gilbert, 1980) is shown on the left including the −10 hexamer of P_{TPCAD} (white bar) and the region of dyad symmetry (solid arrows).

ceptibility of P_{TPCAD} and P_R to in vivo footprinting analysis will be discussed below.

Discussion

We have used in vivo methylation and permanganate footprinting to examine the interaction of the metalloregulatory protein MerR and RNA polymerase at the *mer* regulatory region during repression and induction of the operon. We find, surprisingly, that whether or not the inducer Hg(II) has been added MerR fosters the binding of RNA polymerase at the *mer* structural gene promoter.

Establishment of an Inactive Transcription Complex at P_{TPCAD} under Repression Conditions. The bases in the region of dyad symmetry at P_{TPCAD} whose protection from methylation we ascribe to MerR occupancy are symmetrically placed acrossed two successive major grooves (Figure 9). These bases correspond precisely to those protected by MerR alone in vitro (O'Halloran et al., 1989; Shewchuk et al., 1989b). The observation that MerR-dependent methylation protection in this region does not change significantly upon Hg(II) induction implies that MerR mediates repression and Hg(II)-dependent activation of *merTPCAD* transcription from this one site located between the −10 and −35 regions of P_{TPCAD}. Among well-studied positive activators λ*cII* binds to a site within its target promoters; however, *cII* protects a direct repeat sequence in the −35 promoter region (Ho et al., 1983). LacI when functioning as a transient activator binds well beyond the start point of transcription (Straney & Crothers, 1987). Thus, MerR is unusual among activators in binding within the spacer region between the −10 and −35 recognition hexamers.

Immediately upstream of the positions protected by MerR, several other alterations in DMS reactivity were seen. These DMS reactivity changes [two hyperreactive bases (G −36 and A −37) and a protected G residue at −34 on the bottom strand; see Figure 2] are MerR dependent, and their reactivity is unaltered even in rifampicin-treated cells. Since protection of G −34 can be caused by RNA polymerase (Siebenlist et al., 1980; Kierkegaard et al., 1983; Borowiec & Gralla, 1986; Shanblatt & Revzin, 1986) and since σ-70 interacts, in particular, with the G-C base pair at the third position of the conserved −35 hexamer in P_{ant} and P_{lac} promoters (Gardella et al., 1989), we expected that the strong *mer* P_{TPCAD} down-promoter mutant ($G_{-36}A$) which has less than 1% of wild-type transcriptional activity (Ross et al., 1989) would be lacking in reactivities due to RNA polymerase. Indeed, we found that the mutant $G_{-36}A$ lacks the putative RNA polymerase dependent DMS reactivities seen in the wild-type P_{TPCAD} (Figure 4); however, the methylation changes ascribed to MerR protection were unaltered. Thus, the different methylation patterns of *merOP* in the *merR*$^+$, the *merR*$^-$, and the $G_{-36}A$ backgrounds indicate that, even under conditions when synthesis of *mer* mRNA (Figure 5) and formation of an open complex (Figure 6) are completely undetectable, MerR fosters the binding of RNA polymerase at P_{TPCAD}. In the *glnALG* operon of *E. coli*, σ-54 RNA polymerase binds in a closed complex at the *glnAp2* promoter even with excess nitrogen and irrespective of the presence of NR_I (Kustu et al., 1986; Reitzer et al., 1987; Sasse-Dwight & Gralla, 1988); however in this system, only phosphorylated (active) NR_I causes σ-54 RNA polymerase to form an open complex. To our knowledge, P_{TPCAD} is thus the first example of a σ-70- and activator-dependent transcriptional system in which RNA polymerase is bound at the inactive promoter at a level equivalent to that observed postactivation [Figure 2; compare intensities of G −36 (top), G −34, and A −37 (bottom) before and after addition of Hg(II)].

The observation that RNA polymerase is bound in vivo at the *mer* structural promoter of Tn*21* in the absence of the inducer Hg(II) constrasts with in vitro studies of Tn*501* *mer* transcriptional complexes on linear DNA in which a Hg(II)-treated MerR protein was necessary to obtain RNA polymerase binding at the P_{TPAD} promoter (O'Halloran et al., 1989). The use of linear DNA fragments in the in vitro footprinting strategy may account for the inability of purified RNA polymerase to bind unless Tn*501* MerR had been previously exposed to Hg(II). Alternatively, there may be real differences in the relative promoter strengths of $P_{TP(C)AD}$ and P_R in Tn*21* and Tn*501*, resulting in a preference of RNA polymerase for P_R in Tn*501* until Hg(II) stimulates it to "switch" to occupancy of P_{TPAD} (O'Halloran et al., 1989). Frantz and O'Halloran (1990) have recently found that if the −35 region of Tn*501* P_R is deleted, RNA polymerase will bind along with MerR at P_{TPAD} in vitro in the absence of Hg(II). Footprinting of relevant mutants in the Tn*21* *merOP* region (in progress) or in vivo footprinting of the wild-type Tn*501* system will distinguish whether the differences we observe are technical or biological.

DNA Melting within the mer Operator during Transcriptional Activation. In the presence of Hg(II), initiation of transcription of *merTPCAD* mRNA is accompanied by clear alterations in the DMS reactivities of several bases in P_{TPCAD}. These changes in DMS reactivity occur both within and up- and downstream of the dyadic MerR binding site. Of the residues protected by MerR, only protection of G −18 (nearest to the −10 region; Figures 2, 3, and 9) is diminished, whereas the reactivity of the three other MerR-protected G's is unaltered during induction (Figures 2 and 3). Downstream of the MerR-protected region of P_{TPCAD}, several Hg(II)-induced changes in DMS reactivity occur including protection of G residues at −17, −14, −10, and −9 and a hyperreactive G at position +2 (Figures 2 and 3). In the presence of Hg(II), rifampicin, which is expected to trap RNA polymerase in an open complex, strengthens the protection of G's (−34, −17, −14, −10, and −9; Figures 2 and 3) in the −10 and −35 regions of P_{TPCAD}, suggesting that changes in DMS reactivity outside of the dyadic MerR binding site are caused by RNA polymerase.

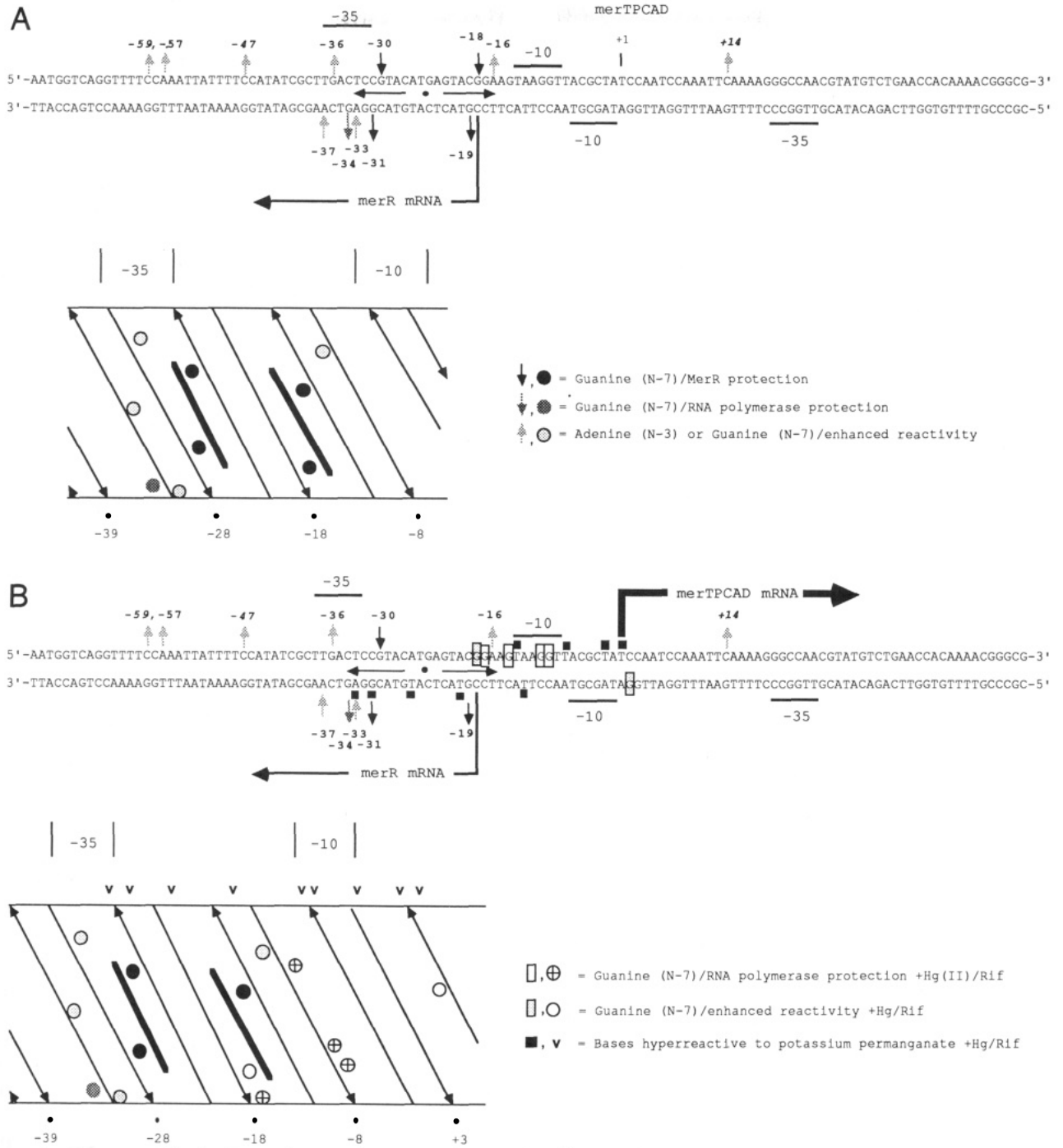

FIGURE 9: Summary of in vivo interactions at the *mer* regulatory region (from position −73 to position +51 with respect to the start site of *merTPCAD* at +1): (A) repression of P_{TPCAD} [without Hg(II)]; (B) activation of P_{TPCAD} [with Hg(II)]. The positions of DMS-hyperreactive cytosine residues (top strand at −59, −47, and +14) are indicated in italics. Thymine residues at +37 and +45 on the bottom strand that exhibited an unusual reactivity toward DMS (see Figure 2) are not included (see text). Below the linear sequence, a cylindrical projection of B-DNA at 10.5 bp per turn (Wang, 1979) shows methylation protection and hyperreactivities of adenines and guanines at P_{TPCAD}. The N-7 of guanine and the N-3 position of adenine are projected onto this cylindrical helix according to their location in the major and minor groove, respectively. Hg(II)-dependent $KMnO_4$-reactive bases are depicted with carets on top of the helix map.

Recall that the RNA polymerase dependent DMS reactions observed in the −35 region of P_{TPCAD} prior to Hg(II) addition change only slightly when P_{TPCAD} is activated by addition of Hg(II). Thus, the MerR/Hg(II)-induced RNA polymerase footprint suggests that RNA polymerase maintains its −35 region contacts and repositions or stabilizes its −10 region contacts during induction. This MerR/Hg(II)-dependent repositioning of RNA polymerase results in the formation of an open complex at P_{TPCAD} as demonstrated by the Hg(II)-dependent melting of bases in the region between −13 and +1 of the *merTPCAD* promoter (Figure 6). The putative RNA polymerase position during Hg(II) induction (Figure 9) is similar (within limits of sequence homologies) to the RNA polymerase position on the *lac* UV5 promoter in vivo (Borowiec & Gralla, 1986) and corroborates the in vitro studies of the MerR/Hg-induced RNA polymerase footprint at the Tn*501 mer* structural gene promoter (O'Halloran et al., 1989).

However, the permanganate reaction patterns of the Hg(II)-induced system display several hyperreactive bases within the dyadic MerR binding site which are not expected to be part of the domain melted by RNA polymerase in an open complex. In other systems examined to date, the open complex

is found between −12 and +2/+4 (O'Halloran et al., 1989; Sasse-Dwight & Gralla, 1988, 1989; Kirkegaard et al., 1983; Siebenlist et al., 1980; Siebenlist, 1979). The unusual in vivo permanganate reactivities which are entirely absent in vitro (O'Halloran et al., 1989) include two T's at −20 and −26 and G −31 and A −33, all on the bottom strand (Figure 6). These results suggest that, upon Hg(II) induction, initiation of *merTPCAD* transcription from P_{TPCAD} is associated with conformational changes in the *mer* operator dyad. Also consistent with a Hg(II)-induced change in this region is a slight deprotection of G −18 (Figures 2, 3, and 9). The dyad permanganate reactivities at T −26, G −31, and A −33 (bottom) do not occur in the activation-deficient mutant $G_{-36}A$, suggesting that their occurrence (which is also lacking in the *merR*Δ strain) depends on a concerted reaction of MerR and RNA polymerase. Further support for the idea of Hg(II)-induced distortion in the dyad region is found in the recent observations of increased in vitro sensitivity to the copper–phenanthroline nuclease of certain bases in this region of Tn*501* (Frantz & O'Halloran, 1990).

Hg(II)-dependent increases in permanganate reactivity do occur in the $G_{-36}A$ mutant at A −2 and T's at −12, −16, −20, −28, and −35 (Figure 7, bottom). Hg(II) alone [but not Hg(II) plus rifampicin] results in similarly increased reactivity at these positions on the bottom strand in both *merR*$^+$ and *merR*Δ (Figure 6, bottom). The consistent appearance of these "Hg(II)-stimulated, rifampicin-dampened" T reactions in all alleles examined suggests that they may arise from direct interaction of the supercoiled DNA with Hg(II) (Gruenwedel & Cruickshank, 1989) or as a general stress-related change in supercoiling (Ni'Bhriain et al., 1989). The preceding interpretation may also explain Hg(II)-stimulated, rifampicin-dampened reactions seen only in the *merR*$^+$ background (Figure 6, bottom strand T −23 and C's −17 and −24). These reactivities depend on RNA polymerase continuously initiating productive *merTPCAD* transcription [i.e., in the presence of Hg(II) alone], but these bases may be "protected" from reacting with permanganate when RNA polymerase is "trapped" at P_{TPCAD} in the presence of rifampicin and Hg(II). The fact that all of the unusual Hg(II)-dependent upstream permanganate reactions occur only on the bottom strand may be due to the involvement of top-strand bases in base pairing to form the *merR* transcript; however, this point remains to be examined. The unusually reactive T −37 (top, Figure 7) position in the $G_{-36}A$ mutant may arise from a MerR-induced distortion detectable only in the absence of RNA polymerase. Alternatively, this region may simply be more easily melted in the mutant as a result of the adjacent G → A transition. Additional genetic and physical studies in progress will resolve this point.

A Model for the Transcriptional Activation of the mer Operon. Our observations suggest a mechanism of transcriptional repression and activation of the *mer* operon in which MerR, bound to the region of dyad symmetry in *merOP*, causes RNA polymerase to occupy an inactive promoter, either by protein–protein interaction or by changing the DNA configuration, or both (Figure 10). That MerR fosters the "prearming" of P_{TPCAD} rather than merely blocking open complex formation is supported by the following observations. First, the lack of an RNA polymerase footprint in the presence of rifampicin in the transcriptionally active *merR*Δ strain (i.e., under conditions expected to freeze RNA polymerase in an open complex at P_{TPCAD}) indicates relative instability without MerR of both the closed and open complexes at P_{TPCAD}. In contrast, when MerR is present, the RNA polymerase methylation footprint (as defined by reactions at A −33 and G −34 and at A −37 bottom and position G −36 top) is evident. Moreover, the reactivity of these bases remains the same both before and after the inducer has been added, and that level of reactivity is considerably higher than the (undetectable) reactivity in the absence of MerR. The constant intensity (pre- and postinducer) of the signals which we ascribe to RNA polymerase indicates that MerR is enhancing the affinity of this region of DNA for RNA polymerase (thus "pre-arming" P_{TPCAD}) while simultaneously preventing RNA polymerase from beginning transcription.

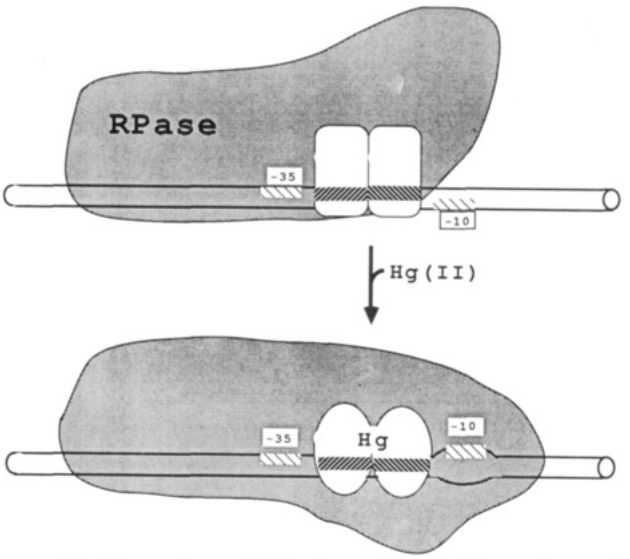

FIGURE 10: Pre-arming model for the regulation of P_{TPCAD} (see text). The functional domains of MerR [C-terminus (shaded) = Hg/activation; N-terminus (black) = DNA binding domain] are indicated according to Ross et al. (1989) and Shewchuk et al. (1989a). In the presence of Hg(II), DNA-bound MerR forms a metal-bridged dimer (Shewchuk et al., 1989c). The concurrent conformational change of MerR believed to occur in the presence of Hg(II) is indicated by different shapes. The alteration in the relative positions of −10 and −35 hexamers and the formation of the open complex are also indicated (see text).

The unique binding site of MerR with respect to RNA polymerase at P_{TPCAD} suggests that MerR might contact RNA polymerase directly. One possibility of direct MerR–RNA polymerase interactions during Hg(II) induction is suggested by recent genetic studies (Ross et al., 1989) which have identified a role in activation of an acidic region of MerR analogous to the acidic "activating patch" found to be important for RNA polymerase interaction in other activator proteins (Bushman & Ptashne, 1988); however, due to MerR's unusual binding site and its interaction with RNA polymerase during repression as well as during activation of P_{TPCAD}, this putative acidic activating region is probably insufficient to account for the complexity of MerR-dependent regulation. That RNA polymerase–DNA interactions are also important is underscored by the behavior of the $G_{-36}A$ mutant, which, while capable of binding MerR, cannot bind RNA polymerase. Once bound, the RNA polymerase is thwarted by the overlong spacer (19 bp) from facile interaction with the −10 region needed to form an open complex. Nonetheless, MerR must also "block" RNA polymerase prior to induction because the transcription of the repressed system is considerably lower than that of the derepressed promoter [Figure 5 and Ross et al. (1989)].

When Hg(II) is added, MerR undergoes a conformational change (Frantz & O'Halloran, 1990; Helmann & Walsh, 1990; O'Halloran et al., 1989; Shewchuk et al., 1989a–c)

which results in the formation of an open complex. MerR's contacts with DNA apparently do not change much during this activity; whether the putative MerR–RNA polymerase contacts change remains to be determined. Clearly, the RNA polymerase contacts with DNA change radically. The present model proposes that in the wild-type system MerR fosters a distortion of the helix (either untwisting or bending) so as to facilitate apposition of the relevant surface of RNA polymerase and the major groove of the −10 region. In other systems, activator-induced bending has been shown to occur when CAP, binding to a site upstream of the −35 region, interacts with the *lac* promoter (Lui-Johnson et al., 1986). In addition, in the A1 promoter of phage T7 and in the *gal* operon, RNA polymerase itself induces bending near the transcriptional initiation points (Kuhnke et al., 1989; Heumann et al., 1988). Alternatively, since the permanganate reactivities (−20 to −33) extend over one full turn of a B-form DNA, they may arise from unwinding of the P_{TPCAD} spacer DNA. This MerR/Hg(II)-mediated repositioning of RNA polymerase would establish a stressed state which is relieved by RNA polymerase melting P_{TPCAD} in an open complex. The formation of a stressed state has previously been proposed in the *lac* promoter system (Borowiec & Gralla, 1986; Stefano & Gralla, 1982). Interestingly, despite the fact that MerR's occupancy of the DNA is unchanged when the $G_{-36}A$ mutant is induced, MerR is apparently unable, in the absence of RNA polymerase, to effect the distortion of the helix (Figure 7). Thus, unlike *lac*, the activation mechanism proposed here involves a concerted activity of MerR–Hg(II) and RNA polymerase.

With respect to P_R, the *merR* promoter also has 19-bp spacing in Tn*21* and, thus, also might be expected to be a relatively weak, free-standing promoter. Nonetheless, under derepressed conditions (pAH1974) when P_R is measureably active (Figure 8), the lack of sharply defined DMS or $KMnO_4$ reactivities, compared to those observed with activated P_{TPCAD}, suggests a relative lack of synchrony in the initiation of transcription at P_R compared to P_{TPCAD}. The preassembled transcription complex at P_{TPCAD} may favor unusually synchronous initiation and correspondingly distinct footprints. Initiation at P_R, like initiation at derepressed P_{TPCAD}, while continuous in vivo, may not be so tightly synchronized by comparison to the in vitro conditions and thus yield less distinct footprints. Alternatively, short half-lives of the RNA polymerase–P_R complex may explain the lack of a distinct footprint at this promoter. Our own observations of Tn*21 mer* mRNA synthesis rates in vivo (B. D. Gambill and A. O. Summers, unpublished results) as well as kinetic measurements of abortive transcription in Tn*501* in vitro (Ralston & O'Halloran, 1990) are consistent with the MerR–RNA polymerase complex being poised for very rapid, Hg(II)-responsive initiation of transcription at $P_{TP(C)AD}$. Current footprinting analysis of our extensive collection of *merR* (Ross et al., 1989) and *merOP* (S.-J. Park and A. O. Summers, unpublished results) mutants will clarify these issues.

ACKNOWLEDGMENTS

We thank Jay Gralla for communicating to us the in vivo potassium permanganate method prior to publication. We also thank Mark Schell for his helpful comments during the course of this work, and we are most grateful to Diane Gambill for assistance in mapping of the *merR* transcript.

REFERENCES

Aiba, H. (1983) *Cell 32*, 141–149.

Auble, D. T., & deHaseth, P. L. (1988) *J. Mol. Biol. 202*, 471–482.

Barrineau, P., Gilbert, P., Jackson, W. J., Jones, C. S., Summers, A. O., & Wisdom, S. (1984) *J. Mol. Appl. Genet. 2*, 601–619.

Borowiec, J. A., & Gralla, J. D. (1986) *Biochemistry 25*, 5051–5057.

Borowiec, J. A., Zhang, L., Sasse-Dwight, S., & Gralla, J. D. (1987) *J. Mol. Biol. 196*, 101–111.

Bushman, F. D., & Ptashne, M. (1988) *Cell 54*, 191–197.

Carpousis, A. J., & Gralla, J. D. (1985) *J. Mol. Biol. 183*, 165–177.

Crosa, J. H., & Falkow, S. (1981) in *Manual of Methods for General Bacteriology* (Gerhardt, P., Murray, R. G. E., Costilow, R. N., Nester, E. W., Wood, W. A., Krieg, N. R., & Phillips, G. B., Eds.) pp 267–281, American Society for Microbiology, Washington, DC.

Foster, T. J. (1987) *Crit. Rev. Microbiol. 115*, 117–140.

Foster, T. J., & Brown, N. L. (1985) *J. Bacteriol. 163*, 1153–1157.

Foster, T. J., Nakahara, H., Weiss, A. A., & Silver, S. (1979) *J. Bacteriol. 140*, 167–181.

Frantz, B., & O'Halloran, T. V. (1990) *Biochemistry 29*, 4747–4751.

Gardella, T., Moyle, H., & Susskind, M. M. (1989) *J. Mol. Biol. 206*, 579–590.

Giniger, E., Varnum, S. M., & Ptashne, M. (1985) *Cell 40*, 767–773.

Green, M., & Roeder, R. G. (1980) *Cell 22*, 231–242.

Gruenwedel, D. W., & Cruikshank, M. K. (1989) *Nucleic Acids Res. 17*, 9075–9086.

Harley, C. B., & Reynolds, R. P. (1987) *Nucleic Acids Res. 15*, 2343–2361.

Hawley, D. K., & McClure, W. R. (1983) *Nucleic Acids Res. 11*, 2237–2255.

Helmann, J. D., & Walsh, C. T. (1990) *Science 247*, 946–948.

Heltzel, A., Gambill, D., Jackson, W. J., Totis, P. A., & Summers, A. O. (1987) *J. Bacteriol. 169*, 3379–3384.

Heltzel, A., Totis, P., & Summers, A. O. (1989) in *Metal Ion Homeostasis: Molecular Biology and Chemistry* (Hamer, D., & Winge, D., Eds.) pp 427–438, Alan R. Liss, New York.

Heumann, H., Ricchetti, M., & Werel, W. (1988) *EMBO J. 7*, 4379–4381.

Ho, Y.-S., Wulff, D. L., & Rosenberg, M. (1983) *Nature 304*, 703–708.

Kirkegaard, K., Buc, H., Spassky, A., & Wang, J. C. (1983) *Proc. Natl. Acad. Sci. U.S.A. 80*, 2544–2548.

Kuhnke, G., Theres, C., Fritz, H.-J., & Ehring, R. (1989) *EMBO J. 8*, 1247–1255.

Kushner, S. R. (1978) in *Genetic Engineering* (Boyer, H. W., & Nicosia, S., Eds.) pp 17–23, Elsevier, Amsterdam, Holland.

Kustu, S., Sei, K., & Keener, J. (1986) in *Regulation of Gene Expression, Symposium of the Society for General Microbiology* (Booth, I., & Higgins, C., Eds.) pp 139–154, Cambridge University Press, New York.

Lawley, P. D., & Brookes, P. (1963) *Biochem. J. 89*, 127–138.

Lee, I. W., Gambill, B. D., & Summers, A. O. (1989) *J. Bacteriol. 171*, 2222–2225.

Lui-Johnson, H.-N., Gartenberg, M. R., & Crothers, D. M. (1986) *Cell 47*, 995–1005.

Lund, P. A., & Brown, N. L. (1987) *Gene 52*, 207–214.

Lund, P. A., Ford, S. J., & Brown, N. L. (1986) *J. Gen. Microbiol. 132*, 465–480.

Maniatis, T., Fritsch, E. F., & Sambrook, J. (1982) *Molecular Cloning: A Laboratory Manual*, Cold Spring Harbor

Laboratory, Cold Spring Harbor, NY.
Maxam, A., & Gilbert, W. (1980) *Methods Enzymol. 65*, 499-560.
McClure, W. R. (1985) *Annu. Rev. Biochem. 54*, 171-204.
Miller, J. H. (1972) *Experiments in Molecular Genetics*, Cold Spring Harbor Laboratory, Cold Spring Harbor, NY.
Misra, T. K., Brown, N. L., Fritzinger, D. C., Pridmore, R. D., Barnes, W. M., Haberstroh, L., & Silver, S. (1984) *Proc. Natl. Acad. Sci. U.S.A. 81*, 5975-5979.
Ni'Bhriain, N. N., Silver, S., & Foster, T. J. (1983) *J. Bacteriol. 155*, 690-713.
Ni'Bhriain, N., Dorman, C. J., & Higgins, C. F. (1989) *Mol. Microbiol. 3*, 933-942.
O'Halloran, T. V., Frantz, B., Shin, M. K., Ralston, D. M., & Wright, J. G. (1989) *Cell 56*, 119-129.
Ralston, D. M., & O'Halloran, T. V. (1990) *Proc. Natl. Acad. Sci. U.S.A. 56*, 3846-3850.
Reitzer, L. J., Bueno, R., Cheng, W. D., Abrams, S. A., Rothstein, D. M., Hunt, T. P., Tyler, B., & Magasanik, B. (1987) *J. Bacteriol. 169*, 4279-4284.
Ross, W., Park, S.-J., & Summers, A. O. (1989) *J. Bacteriol. 171*, 4009-4018.
Sasse-Dwight, S., & Gralla, J. D. (1988) *Proc. Natl. Acad. Sci. U.S.A. 85*, 8934-8938.
Sasse-Dwight, S., & Gralla, J. D. (1989) *J. Biol. Chem. 264*, 8074-8081.
Shanblatt, S. H., & Revzin, A. (1986) *J. Biol. Chem. 261*, 10885-10890.
Shewchuk, L. M., Helmann, J. D., Ross, W., Park, S.-J., Summers, A. O., & Walsh, C. T. (1989a) *Biochemistry 28*, 2340-2344.
Shewchuk, L. M., Verdine, G. L., & Walsh, C. T. (1989b) *Biochemistry 28*, 2331-2339.
Shewchuk, L. M., Verdine, G. L., Nash, H., & Walsh, C. T. (1989c) *Biochemistry 28*, 6140-6145.
Siebenlist, U. (1979) *Nature 279*, 651-652.
Siebenlist, U., Simpson, R. B., & Gilbert, W. (1980) *Cell 20*, 269-281.
Sippel, A., & Hartmann, G. (1968) *Biochim. Biophys. Acta 157*, 218-219.
Stefano, J. E., & Gralla, J. D. (1982) *Proc. Natl. Acad. Sci. U.S.A. 79*, 1069-1072.
Straney, S. B., & Crothers, D. M. (1987) *Cell 51*, 699-707.
Summers, A. O. (1986) *Annu. Rev. Microbiol. 40*, 607-634.
Walsh, C. T., Distefano, M. D., Moore, M. J., Shewchuk, L. M., & Verdine, G. L. (1988) *FASEB J. 2*, 124-130.
Wang, C. W. (1979) *Proc. Natl. Acad. Sci. U.S.A. 76*, 200-203.

Replacement of a Labile Aspartyl Residue Increases the Stability of Human Epidermal Growth Factor†

Carlos George-Nascimento,*,‡ Jonathan Lowenson,§ Michael Borissenko,‡ María Calderón,‡ Angélica Medina-Selby,‡ Jane Kuo,‡ Steven Clarke,§ and Anne Randolph‡

Chiron Research Laboratories, Chiron Corporation, Emeryville, California 94608, and Department of Chemistry and Biochemistry and Molecular Biology Institute, University of California, Los Angeles, California 90024

Received May 2, 1990; Revised Manuscript Received July 20, 1990

ABSTRACT: Long-term storage of recombinant human epidermal growth factor (EGF), an important promoter of cell division, results in its conversion to a new species that elutes later than native EGF on a reverse-phase column. This new species, called EGF-X, has only 20% of the biological activity of native EGF. Peptide mapping indicated that the primary structure of EGF-X differs from that of native EGF solely within the first 13 residues. N-Terminal sequencing of EGF-X revealed that about 30% of the polypeptides have been cleaved at the Asp-3/Ser-4 bond. In addition, the yields after the His residue at position 10 were extremely low, indicating that a chemical modification occurs at residue 11 that is incompatible with Edman degradation. We hypothesized that aspartic acid 11 had been converted to an isoaspartyl residue, and this was confirmed with L-isoaspartyl/D-aspartyl methyltransferase, an enzyme that methylates the side-chain carboxyl group of L-isoaspartyl residues but does not recognize normal L-aspartyl residues. EGF-X, but not EGF, was found to be a substrate of this enzyme, and proteolytic digestion of EGF-X with thermolysin localized the site of methylation to a nine-residue peptide containing position 11. We did not observe formation of the isoaspartyl derivative in EGF that had been denatured by reduction of its disulfide bonds. In addition, replacement of the aspartyl residue at position 11 with glutamic acid resulted in a fully active EGF derivative that does not form detectable amounts of EGF-X. We propose that conversion of this aspartyl residue to isoaspartate is a significant nonenzymatic degradation reaction affecting this growth factor. Replacing this residue with a glutamyl residue, however, prevents this degradation reaction, producing a biologically active EGF molecule with greater stability.

Epidermal growth factor (EGF)[1] is a potent mitogen and an inhibitor of gastric acid secretion. Due to these biological activities, EGF has been studied extensively since its discovery (Cohen, 1962). Human EGF has 53 amino acid residues and three disulfide bridges, the positions of which are conserved

† This work was partially supported by a grant from the National Science Foundation (DMB 89-04170) to S.C. and a U.S. Public Health Training Grant (GM 07185) to J.L.

‡ Chiron Corp.
§ University of California.

[1] Abbreviations: EGF, epidermal growth factor; HPLC, high-performance liquid chromatography; IAA, iodoacetic acid; D11E-EGF, variant of epidermal growth factor having glutamic acid at position 11.

0006-2960/90/0429-9584$02.50/0